Molecular Pharmacology Fast Forward. Published on April 14, 2006 as doi:10.1124/mol.106.023275
This article has not been copyedited and formatted. The final version may differ from this version.

MOL 23275

Structure-function analysis of vitamin D 24-hydroxylase (CYP24A1) by site-directed mutagenesis: amino acid resides responsible for species-based difference of CYP24A1 between humans and rats

Hiromi Hamamoto, Tatsuya Kusudo, Naoko Urushino, Hiroyuki Masuno, Keiko Yamamoto, Sachiko Yamada, Masaki Kamakura, Miho Ohta, Kuniyo Inouye, Toshiyuki Sakaki

Division of Food Science and Biotechnology, Graduate School of Agriculture, Kyoto University, Sakyo-ku, Kyoto 606-8502, Japan: H.H., T.K., N.U., K.I.
Institute of Biomaterials and Bioengineering, Tokyo Medical and Dental University, 2-3-10 Kanda-Surugadai, Chiyoda-ku, Tokyo 101-0062, Japan: H.M., K.Y., S.Y.
Biotechnology Research Center, Faculty of Engineering, Toyama Prefectural University, 5180 Kurokawa, Kosugi, Toyama 939-0398, Japan: M.K., T.S.
Laboratory of Nutrition, Koshien College, 4-25 Kawarabayashi-cho, Nishinomiya, 663-8107, Japan: M.O.

Molecular Pharmacology Fast Forward. Published on April 14, 2006 as DOI: 10.1124/mol.106.023275
This article has not been copyedited and formatted. The final version may differ from this version.

MOL 23275

Running title: Structure-function analysis of CYP24A1

Corresponding author: Toshiyuki Sakaki
Biotechnology Research Center,
Faculty of Engineering, Toyama Prefectural University,
5180 Kurokawa, Imizu, Toyama 939-0398, Japan
Phone:+81-766-56-7500 Ext.567
Fax: +81-766-56-2498
E-mail: tsakaki@pu-toyama.ac.jp

Text page: 21
Table: 3
Figure: 8
Reference: 37
Abstract: 161 words
Introduction: 571 words
Discussion: 1009 words

Abbreviations

The abbreviations used are : VDDRI, vitamin D-dependent rickets type I; 1α,25$(OH)_2D_3$, 1α,25-dihydroxyvitamin D_3; ADR, NADPH-adrenodoxin reductase

Molecular Pharmacology Fast Forward. Published on April 14, 2006 as DOI: 10.1124/mol.106.023275
This article has not been copyedited and formatted. The final version may differ from this version.

Abstract

Our previous studies revealed the species-based difference of CYP24A1- dependent vitamin D metabolism. Although human CYP24A1 catalyzes both C-23 and C-24 oxidation pathways, rat CYP24A1 shows almost no C-23 oxidation pathway. We tried to identify amino-acid residues that cause the species-based difference by site-directed mutagenesis. In the putative substrate-binding regions, amino-acid residue of rat CYP24A1 was converted to the corresponding residue of human CYP24A1. Among eight mutants examined, T416M and I500T showed C-23 oxidation pathway. In addition, the mutant I500F showed quite a different metabolism of $1\alpha,25(OH)_2D_3$ from both human and rat CYP24A1. These results strongly suggest that the amino-acid residues at positions 416 and 500 play a crucial role in substrate-binding, and greatly affect substrate orientation. A three-dimensional model of CYP24A1 indicated that the A-ring and triene part of $1\alpha,25(OH)_2D_3$ could be located close to amino acid residues at positions 416 and 500, respectively. Our findings provide useful information for the development of new vitamin D analogs for clinical use.

Molecular Pharmacology Fast Forward. Published on April 14, 2006 as DOI: 10.1124/mol.106.023275
This article has not been copyedited and formatted. The final version may differ from this version.

Introduction

The hormonally active form of vitamin D_3, $1\alpha,25(OH)_2D_3$, plays essential roles in calcium homeostasis, immune response, and cell differentiation (Norman *et al*., 1971, Lawson *et al*., 1971, Holick *et al*., 1971, Bouilon *et al*., 1995). A large number of vitamin D analogs have been synthesized for clinical use in type I rickets, osteoporosis, renal osteodystrophy, psoriasis, leukemia and breast cancer, and their biological activity has been evaluated. Much research has investigated the the biological activity mechanism of vitamin D analogs, revealing that the biological activities of analogs are not only due to the analog itself but also its metabolites (Binderup et al., 1991, Binderup, 1992, Dilorth et al., 1997). CYP24A1 plays a central role in the metabolism of $1\alpha,25(OH)_2D_3$ and its analogs in target tissues such as kidneys, intestines and bones. Recently, a species-based difference was revealed in the CYP24A1-dependent metabolism of $1\alpha,25(OH)_2D_3$ between rats and humans (Akiyoshi-Shibata *et al*., 1994, Beckman *et al*., 1996, Sakaki *et al*., 1999, Sakaki *et al*., 2000). Human CYP24A1 demonstrated a remarkable metabolism consisting of both C-23 and C-24 oxidation pathways, while rat CYP24A1 showed extreme predominance of C-24 over C-23 oxidation pathways. In addition, a remarkable species-based difference was also observed in the CYP24A1-dependent metabolism of vitamin D analogs (Sakaki *et al*., 2003, Kusudo *et al*., 2003, Kusudo *et al*., 2004, Abe *et al*., 2005). These facts suggest that pre-clinical tests using such animals as rats and mice cannot correctly predict the metabolism of vitamin D analogs in the human body. Thus, information on substrate recognition, the reaction mechanism and the species-based difference of CYP24A1 appears quite useful to develop vitamin D analogs for clinical use. Another areas of CYP24A1 research with pharmacological interest is development of specific inhibitor of CYP24A1 (Schuster et al., 2003, Kahraman *et al*., 2004). Blockers of CYP24A1 might extend the half-life of $1\alpha,25(OH)_2D_3$ and its analogs within target cells, especially cells that overexpress CYP24A1. Also in this case, information on tertiary structure of substrate-binding pocket of CYP24A1 is quite useful to develop specific inhibitor of CYP24A1. Recently, tertiary structure of CYP24A1 was proposed by molecular modeling (Omdahl et al., 2003).

So far, crystal structures of more than ten prokaryotic CYPs and four mammalian microsomal CYPs have been solved (Williams *et al*., 2000, Williams *et al*., 2003, Scott *et al*., 2003, Wester *et al*., 2003, Williams *et al*., 2004, Schoch *et al*., 2004, Yano *et al*., 2005, Rowland *et al*., 2006). The overall folding of those CYPs is quite similar, although their sequence identity is less than 20%. These findings strongly suggest that mitochondrial CYPs have similar structural folding to prokaryotic soluble and microsomal CYPs. Recently, we constructed tertiary structure of CYP27B1 by a homology modeling technique using the structure of CYP2C5 as a template (Yamamoto *et al*., 2004, Yamamoto *et al*., 2005). The

resultant three-dimensional model of CYP27B1 provided an opportunity to understand the spatial location and function of the residues responsible for mutations with vitamin D-dependent rickets type I (VDDR-I). Using the three-dimensional model we studied the docking of 25-hydroxyvitamin D_3 into the substrate-binding pocket of CYP27B1, and predicted that Thr409 of human CYP27B1 is responsible for substrate binding. Thus, a homology modeling technique together with mutation study gives useful information on the structure-function analysis of mitochondrial CYPs.

In this study, we attempted to construct three-dimensional model of CYP24A1 to understand structure-function relationship of CYP24A1. The enzymatic properties of CYP24A1 mutants constructed by site-directed mutagenesis were examined to determine the amino acid residues responsible for the species-based difference of CYP24A1 between humans and rats.

Molecular Pharmacology Fast Forward. Published on April 14, 2006 as DOI: 10.1124/mol.106.023275
This article has not been copyedited and formatted. The final version may differ from this version.

Materials and methods

Materials

DNA modifying enzymes and restriction enzymes were purchased from Takara Shuzo Co., Ltd. (Kyoto, Japan). 1α,25(OH)$_2$D$_3$ was purchased from Wako Pure Chemical Industries, Ltd. (Osaka, Japan). NADPH was purchased from Oriental Yeast Co. (Tokyo, Japan). Bovine NADPH-adrenodoxin reductase (ADR) and adrenodoxin were kindly given by Dr. Y. Nonaka (Koshien University). Terrific broth was purchased from Gibco BRL (Paisley, UK). *Escherichia coli* JM109 (Takara Shuzo, Kyoto, Japan) was used as a host strain. Other chemicals used were of the highest quality commercially available.

Sequence alignment and Homology modeling

Rat CYP24A1, human CYP24A1 and rabbit microsomal CYP2C5 were aligned by using ClustalW interfaced with Clustal X (ver 1.81) for Windows. According to the alignment, we constructed three-dimensional models of human CYP24A1 and rat CYP24A1 by using SYBYL modeling software, COMPOSER (Tripos Inc.), and the atomic coordinate of the crystal structure of rabbit CYP2C5 as a template (Williams et al., 2000, Wester et al., 2003). Modeling procedures were summarized below.

1. The structure of the structurally conserved regions (SCR) (all helices, β-sheets, and loops having the same number of amino acid residues) was constructed.
2. Backbone structure of the residual parts was constructed with the loop search command of SYBYL and the selected loops were joined to the SCR parts; then their side chains were added.
3. Heme was merged into the protein as it adopts the same spatial location as the heme of the template CYP2C5.
4. Hydrogens were added to the model structure.
5. The constructed structure was optimized in added water by the precomputed box method (Tripos force field). Optimization was carried out in the following order of consideration: loop regions, side chains, and the whole molecule. Each energy minimization was carried out 5000 iterations. The model structure was evaluated by PROCHECK Program.
6. 1α,25(OH)$_2$D$_3$ was manually docked into CYP24A1 model based on the experimental results of site-directed mutagenesis described below.

Substrate docking

The substrate, 1α,25(OH)$_2$D$_3$, was manually docked into CYP24A1 model based on experimental results of the site-directed mutagenesis.

1. 1α,25(OH)$_2$D$_3$ was put into the substrate binding pocket, as the triene part was located near

Molecular Pharmacology Fast Forward. Published on April 14, 2006 as DOI: 10.1124/mol.106.023275
This article has not been copyedited and formatted. The final version may differ from this version.

the important residues, I500 and T416, for regioselectivity of the side-chain hydroxylation and C(23)- and C(24)-positions of the side chain were near the Fe of the heme.

2. Optimization of the resultant docking model was performed on the Tripos force field, in which the protein part was fixed.
3. We selected one 1α,25$(OH)_2D_3$-CYP24A1 complex model in which 1α,25$(OH)_2D_3$ adopted its stable conformation.

Site-directed mutagenesis.

The mutated amino acid residues and their putative locations are summarized in Table 1. Mutants were generated by Quik Change™ Site-directed Mutagenesis kit (Stratagene) according to the instruction manual. The oligonucleotide primers for mutagenesis are shown in Table 2. Corrected generation of desired mutations was confirmed by DNA sequencing.

Cultivation of the recombinant E. coli cells

Recombinant *E. coli* cells were grown in TB broth containing 50 μg/ml ampicillin at 26℃ under good aeration. The induction of transcription of CYP24A1 cDNA under tac promoter was initiated by addition of isopropyl-thio-β-D-garactopyranoside (IPTG) at final concentration of 1 mM when the cell density (O.D.660) reached 0.5. δ-Aminolevulinic acid was also added at a final concentration of 0.5 mM. The recombinant cells were gently shaken at 26℃ under good aeration by bubbling as described previously (Akiyoshi-Shibata *et al*., 1994).

Preparation of membrane fraction

Subcellular fractionation of *E. coli* cells was carried out basically according to our previous study (Akiyoshi-Shibata *et al*., 1994). 100 mM Tris-HCl (pH 7.4) buffer was used for suspension of the membrane fraction.

Measurement of reduced CO difference spectra

The reduced CO-difference spectra were measured with a Shimadzu UV-2200 spectrophotometer (Kyoto, Japan) (Omura and Sato, 1994, Kondo *et al*., 1999). The absorption-coefficient difference between 445 nm and 490 nm ($\Delta \varepsilon_{445\text{-}490}$)=105 $mM^{-1}cm^{-1}$ was used for the calculation of the P450 hemoprotein concentration, as described previously (Akiyoshi-Shibata *et al*., 1994).

Measurement of enzyme activity of CYP24A1

The activity towards 1α,25$(OH)_2D_3$ was measured in the reconstituted system containing the

Molecular Pharmacology Fast Forward. Published on April 14, 2006 as DOI: 10.1124/mol.106.023275
This article has not been copyedited and formatted. The final version may differ from this version.

membrane fraction 10-30 nM of CYP24A1, 2 μM of adrenodoxin, 0.2 μM of NADPH-adrenodoxin reductase (ADR), 4 μM substrate, 100 mM Tris-HCl (pH 7.4) and 1 mM EDTA in a final volume of 0.5 ml. For the determination of apparent kinetic parameters, the reaction mixture consisting of the membrane fraction containing 10-30 nM of CYP24A1 or its mutant, 0.1 μM of ADERENODOXIN, 0.01 μM of ADR, 0-2.0 μM of 1α,25$(OH)_2D_3$. To determine K_m values correctly, the successive reaction by CYP24A1 should be avoided as described previously (Sakaki *et al*., 2000, Kusudo *et al*., 2004). Thus, the concentrations of ADERENODOXIN and ADR were extremely reduced. Under these conditions, the sum of 23*S*-hydroxylated and 24*R*-hydroxylated products of the substrate is more than 90 % of total metabolites. The reaction was initiated by adding NADPH to a final concentration of 1 mM. Aliquots of the reaction mixture were collected after varying time intervals and extracted with four volumes of chloroform-methanol (3:1). The organic phase was recovered and dried up. The resulting residue was solubilized with acetonitrile and applied to HPLC under the following conditions: column, YMC-Pack ODS-AM (4.6×300mm) (YMC Co., Tokyo, Japan). UV detection, 265 nm; flow rate, 1.0ml/min; column temperature, 40 ℃; mobile phase, a linear gradient from 20% to 100% acetonitrile in aqueous solution. The metabolites were also analyzed using a JASCO Finepak SIL-5 column (4.0×25 mm)(JASCO Co. Tokyo, Japan).

LC-MS analysis of the metabolites

Isolated metabolites from HPLC effluents were subjected to mass spectrometric analysis using a Finnegan Mat TSQ-70 with atmospheric pressure chemical ionization, positive mode. The conditions of LC were described below: column, reverse phase ODS column (μBondapak C18, 5 μm, Waters) (6 mm x 150 mm); mobile phase, 80% methanol aqueous solution per 25 min; flow-rate, 1.0 mL min^{-1}; UV detection, 265 nm.

Other methods

The concentration of vitamin D_3 derivatives was estimated by their molar extinction coefficient of 1.80 x 10^4 $M^{-1}cm^{-1}$ at 264 nm (Hiwatashi *et al*., 1982). Protein concentration was determined by the method of Lowry *et al.* (1951), using bovine serum albumin as a standard.

Molecular Pharmacology Fast Forward. Published on April 14, 2006 as DOI: 10.1124/mol.106.023275
This article has not been copyedited and formatted. The final version may differ from this version.

Results

Expression of the mutants of rat CYP24A1 in E. coli cells

To determine the amino acid residues responsible for species-based difference of CYP24A1 between humans and rats, their amino acid sequences were compared. Fig. 1 shows the alignment of amino acid sequences of human CYP24A1, rat CYP24A1, and CYP2C5, in which substrate recognition sites (SRS) proposed by Gotoh (1992) were indicated. The amino acid residues not conserved in both CYP24A1 in SRS regions were marked in Fig. 1. The 7 amino acid residues of rat CYP24A1 were each mutated to the corresponding residues of human CYP24A1. Thus, the mutants H125Y, H140Y, N142K, R262S, A270D, L498S, and I500T were expressed in *E. coli* cells. In addition, mutants at 416 position were also constructed because Thr416 of rat CYP24A1 and Met 416 of human CYP24A1 appeared to be close to A-ring of 1α,25(OH)$_2$D$_3$ based on the computer modeling. It should be noted that Thr416 corresponds to Thr409 of human CYP27B1 which is responsible for substrate-binding and whose mutation causes vitamin D-dependent rickets type I (Yamamoto *et al*., 2005). The expression level of human CYP24A1, rat CYP24A1, and its mutants except for T416M, T416V, and N142K was 50-100 nmol/L culture, whereas the expression level of T416M, T416V, and N142K was 15-30 nmols/L culture. All of the wild type and mutants CYP24A1 showed similar reduced CO-difference spectra with a maximum at around 445 nm.

Metabolism of 1α,25(OH)$_2$D$_3$ by human CYP24A1, rat CYP24A1, and its mutants

The reconstituted system containing the membrane fraction prepared from the recombinant *E. coli* cells expressing wild type or mutant CYP24A1, bovine ADERENODOXIN, and bovine ADR was examined for the metabolism of the 1α,25(OH)$_2$D$_3$. Fig. 2 shows metabolic pathways of 1α,25(OH)$_2$D$_3$ catalyzed by CYP24A1 (Sawada *et al*., 2004). Fig. 3 shows HPLC profiles of 1α,25(OH)$_2$D$_3$ and their metabolites by human CYP24A1, rat CYP24A1 and its mutants. Based on our previous data on the metabolism of 1α,25(OH)$_2$D$_3$, the metabolites designated as M1, 2, 3, 4, 5, 6 and 7 were considered to be 1α,23S,25,26(OH)$_4$D$_3$ (M1), 24-oxo-1,23,25(OH)$_3$D$_3$ (M2), 24,25,26,27-tetranor-1,23(OH)$_2$D$_3$ (M3), 1α,23S,25(OH)$_3$D$_3$(M4), 1α,24R,25(OH)$_3$D$_3$(M5), 24-oxo-1,25(OH)$_2$D$_3$ (M6) and 25,26,27-trinor-23-ene-1α(OH)D$_3$ (M7) (Figs.2 and 3). Note that the metabolites of C-23 oxidation pathway, M1 and M7, were detected in the metabolism by the mutants T416M and I500T (Figs. 3-C and 4-B). These results suggest that these mutants have the enzymatic properties similar to human CYP24A1. On the other hand, the mutants H125Y, H140Y, N142Y, R242S, A270D, and L498S showed nearly the same metabolism as rat CYP24A1. Table 2 shows the ratio between summed products of C-23 oxidation pathway (M1, M4, and

Molecular Pharmacology Fast Forward. Published on April 14, 2006 as DOI: 10.1124/mol.106.023275
This article has not been copyedited and formatted. The final version may differ from this version.

M7) and those of C-24 oxidation pathway (M2, M3, M5 and M6) of metabolism by human CYP24A1, rat CYP24A1, and its mutants. The mutants H125Y, H140Y, N142K, R262S, A240D, and L498S showed the same C-23/C-24 ratio, 0.01, as wild type of rat CYP24A1. However, it was demonstrated that single amino acid substitution at 416 or 500 can dramatically increase the ratio of the C-23 to C-24 oxidation pathways (Table 2).

Molecular Modeling of CYP24A1

The overall folding of both rat CYP24A1 and human CYP24A1 was quite similar to those of CYP2C5 used as a template (Williams *et al*., 2000, Wester *et al*., 2003) and three-dimensional model of CYP27B1 in our previous study (Yamamoto *et al*., 2004, Yamamoto *et al*., 2005) (Fig.5). We evaluated the model structures by using the PROCHEK program. Ramachandran plots of rat and human CYP24A1 showed 99% and 97% of residues either in the most favored or allowed regions, respectively. The putative structure of the active center of rat CYP24A1 was shown in Fig. 5. The A-ring and the triene part were located near the amino acid residues Thr416 and Ile500, respectively. The distance between oxygen atom at the side chain of Thr 416 and oxygen atom at C-3 position of 1α,25$(OH)_2D_3$ was estimated to be 6.9 Å, suggesting that no hydrogen bond was formed between both oxygen atoms. The distances between Cδ of Ile 500 and C-7, C-8, and C-19 of 1α,25$(OH)_2D_3$ were estimated to 3.6, 3.5 and 3.4 Å, respectively.

Metabolism of 1α,25$(OH)_2D_3$ by Thr416 mutants

Fig. 3 shows HPLC profiles of 1α,25$(OH)_2D_3$ and their metabolites by Thr416 mutants. The metabolites of C-23 oxidation pathway, M1 and M7, were detected in the metabolism by the mutant T416M corresponding to human CYP24A1. In addition, the mutants T416V, T416M, T416I, and T416F had reaction specificity similar to human CYP24A1. In contrast, the metabolic pattern by the mutants T416A and T416S remains rat CYP24A1 type. Table 3 shows kinetic parameters of Thr416 mutants. The mutants T416A and T416S showed nearly the same K_m and k_{cat} values as the wild type. On the other hand, T416M and T416V whose enzymatic properties are similar to human CYP24A1 (Table 3) showed somewhat larger K_m values than human CYP24A1.

Metabolism of 1α,25$(OH)_2D_3$ by Ile500 mutants

Fig. 3 shows HPLC profiles of 1α,25$(OH)_2D_3$ and their metabolites by Ile500 mutants. The metabolites of C-23 oxidation pathway, M1 and M7, were detected in the metabolism by the mutants I500V, I500A, I500L, suggesting that these mutants had reaction specificity similar to human CYP24A1. In contrast, the metabolic pattern by the mutant I500F was quite different

Molecular Pharmacology Fast Forward. Published on April 14, 2006 as DOI: 10.1124/mol.106.023275
This article has not been copyedited and formatted. The final version may differ from this version.

from those of both human and rat CYP24A1. Normal-phase HPLC analysis demonstrated novel products with one hydroxyl group (Fig. 6). Mass spectrum of the metabolite UK2 is similar to that of 1α,24*R*,25(OH)$_3$D$_3$ with a small difference. Relative intensities (%) of major ion fragments of UK2 were as follows: m/z 361 (M+H-4H$_2$O), 13 %; m/z 379 (M+H-3H$_2$O), 95 %; m/z 397 (M+H-2H$_2$O), 100%; m/z 415 (M+H-H$_2$O), 87 %; m/z 433 (M+H), 4.4 %. On the other hand, relative intensities (%) of major ion fragments of 1α,24*R*,25(OH)$_3$D$_3$. were as follows: m/z 361 (M+H-4H$_2$O), 14 %; m/z 379 (M+H-3H$_2$O), 92 %; m/z 397 (M+H-2H$_2$O), 100%; m/z 415 (M+H-H$_2$O), 117 %; m/z 433 (M+H), 6.9 %. Judging from its retention time in the reversed-phase HPLC, this metabolite is neither 26- nor 27-hydroxylated product. Although the first metabolite in C-24 oxidation pathway, 1α,24*R*,25(OH)$_3$D$_3$(M5), was observed, other metabolites of the C-24 oxidation pathway such as M2, M3 and M6 were not detected. On the C-23 oxidation pathway, 1α,23*S*,25(OH)$_3$D$_3$(M4) and the putative 1α,23*S*,25,26(OH)$_4$D$_3$ (M1) were observed. However, the metabolite 25,26,27-trinor-23-ene-1α(OH)D$_3$ (M7) was not detected. These results strongly suggest that the amino acid residue at position 500 plays a crucial role in substrate-binding.

Molecular Pharmacology Fast Forward. Published on April 14, 2006 as DOI: 10.1124/mol.106.023275
This article has not been copyedited and formatted. The final version may differ from this version.

Discussion

CYP24A1 plays a central role in the metabolism of vitamin D and its analogs in such target tissues as kidneys, intestines and bones. Recently, we revealed the species-based difference on the CYP24A1-dependent metabolism of 1α,25$(OH)_2D_3$ (Sakaki *et al*., 1999, Sakaki *et al*., 2000) and its analogs (Sakaki *et al*., 2003, Kusudo *et al*., 2003, Kusudo *et al*., 2004, Abe *et al*.,2005). Thus, information on substrate recognition, and the reaction mechanism of CYP24A1 appears quite important for the development of vitamin D analogs for clinical use. Recently, Annalora *et al*. (2004) reported the role of Phe249 of rat CYP24A1 in substrate binding. However, this amino acid residue is conserved in rat and human CYP24A1. In this study, we attempted to identify the amino acid residues of responsible for the species-based difference between rat and human CYP24A1.

Recently, we found that CYP3A4 shows 23 and 24-hydroxylation activity toward 1α,25$(OH)_2D_3$ (Xu *et al*., 2006). However, we did not choose CYP3A4 as a template for the construction of a CYP24A1 model for the reasons described below. Although CYP3A4 shows hydroxylation activity toward a large number of compounds with different structures, CYP24A1 shows no activity toward almost all substrates of CYP3A4. CYP3A4 shows non Michaelis-Menten kinetics and both homotropic and heterotrophic cooperativity towards many substrates, suggesting that it has a noncatalytic effector site within the active site cavity. On the other hand, no reports showing atypical kinetic behaviors of CYP24A1 have been published. These results suggest that the substrate recognition of CYP3A4 is quite different from CYP24A1. Substrate specificities of CYP2A6 (Yano *et al*., (2005)), 2B4 (Scott *et al*., (2003)), and 2D6 (Rowland *et al*., (2006)) are quite different from CYP24A1. Thus, we did not choose these CYPs as a template. Since rat CYP2C11 shows 25-hydroxylation activity toward vitamin D_3 (Hayashi *et al*., 1986), it is reasonable to consider that P450s in CYP2C family, CYP2C5 (Williams *et al*., 2000), 2C8 (Schoch *et al*., (2004)), and 2C9 (Williams *et al*., 2003), could be template candidates for the construction of a CYP24A1 model. Our recent report indicates that a CYP27B1 model constructed using CYP2C5 as a template can fully explain our experimental data (Yamamoto *et al*., (2005)). In addition, a CYP27A1 model constructed in a similar way can explain our experimental data (unpublished results). Note that CYP24A1 has a closer evolutionary relationship to CYP27A1 and CYP27B1 than any other CYPs (Nelson *et al*., (2004)). Recently, we revealed that CYP27B1 shows 25-hydroxylation activity toward vitaminD_3 in addition to 1α-hydroxylation activity (Uchida *et al*., (2004)). Thus, CYP27A1, CYP27B1, and CYP24A1 can add a hydroxyl group at the side chain of vitamin D_3. Based on these facts, it is possible to assume that the tertiary structure of CYP24A1 resembles those of CYP27A1 and CYP27B1. Thus, in this study, we chose CYP2C5 as a template for the construction of a CYP24A1 model.

Molecular Pharmacology Fast Forward. Published on April 14, 2006 as DOI: 10.1124/mol.106.023275
This article has not been copyedited and formatted. The final version may differ from this version.

Our previous study on the metabolism of the A-ring diastereomers of 1α,25(OH)$_2$D$_3$ suggested that amino acid residues interacting with the A-ring of the substrate contributed to species-based difference between rat and human CYP24A1 (Kusudo *et al*., 2004). In addition, our recent studies revealed that Thr409 of CYP27B1 is responsible for substrate binding probably because of hydrogen bond formation between the OH group of Thr409 and 25(OH) group of 1α,25(OH)$_2$D$_3$ (Yamamoto *et al*., 2005). Amino acid sequence alignments indicated that Thr416 of rat CYP24A1, and Met416 of human CYP24A1 correspond to Thr409 of human CYP27B. Although the substrate is inserted in an opposite direction between CYP27B1 and CYP24A1, we examined whether Thr416 is involved in substrate binding. The docking model of CYP24A1 and 1α,25(OH)$_2$D$_3$ indicated that the A-ring of 1α,25(OH)$_2$D$_3$ could be located close to the amino acid residue at position 416. Thus, we expressed T416M in *E. coli* cells, and examined its enzymatic properties. As expected, the metabolic pattern of 1α,25(OH)$_2$D$_3$ by mutant T416M resembled human CYP24A1. The ratio of C-23 to C-24 oxidation pathway on T416M was estimated to be 0.08, which was much higher than the wild type of rat CYP24A1 (0.01). Note that animal species with a high ratio of C-23 to C-24 oxidation pathway, such as chicks, and humans have Met at position 416 while those with low C-23 ratio such as rats and mice have Thr at position 416 (Portale and Miller, 2000).

Although Thr 416 is closed to the A-ring, judging from the distance (6.9 Å) between both oxygen atoms, no hydrogen bond can be formed between the oxygen atom on the side chain of Thr 416 and the oxygen atom at the C-3 position of 1α,25(OH)$_2$D$_3$ (Fig. 5). Both T416S and T416A showed only C-24 pathway (rat type) with nearly the same affinity for 1α,25(OH)$_2$D$_3$ as the wild type. On the other hand, Thr416 mutants replaced by such large and hydrophobic amino acids as Met, Val, Ile, and Phe showed both C-23 and C-24 oxidation pathways (human type). The fact that T416V showed human-type metabolism demonstrates that a difference between the hydroxyl group (Thr) and the methyl group (Val) determines the metabolic pattern of 1α,25(OH)$_2$D$_3$. At the present stage, we cannot clearly explain these results from the complex model of CYP24A1 and 1α,25(OH)$_2$D$_3$. However, it might possible to assume that a few water molecules form a hydrogen-bond network between the OH group of the amino acid at position 416 and 3β-OH group of 1α,25(OH)$_2$D$_3$. The hydroxyl group of Thr or Ser is involved in the hydrogen-bond network. Based on the speculations that Ala cannot remove a putative water molecule bound to the 3β-OH group of 1α,25(OH)$_2$D$_3$ whereas Met, Val, Ile, and Phe remove the water molecule to disrupt the hydrogen-bond network, the mutation to the larger hydrophobic residues and removal of water appear to be associated with the shift in metabolism down the C-23 pathway.

Of the seven mutants in the SRS regions (Fig. 1), only I500T showed human-type metabolic pattern. Based on the three-dimensional model of rat CYP24A1, Ile 500 was located near the

Molecular Pharmacology Fast Forward. Published on April 14, 2006 as DOI: 10.1124/mol.106.023275
This article has not been copyedited and formatted. The final version may differ from this version.

triene part of 1α,25(OH)$_2$D$_3$. The distances between Cδ of Ile 500 and C-7, C-8, and C-19 of 1α,25(OH)$_2$D$_3$ were estimated to 3.6, 3.5 and 3.4 Å, respectively (Fig. 5). In addition to I500T, mutants I500A, I500V, and I500L also showed a metabolic pattern similar to human CYP24A1. These results reveal that rat CYP24A1-type metabolism is specifically observed when the amino acid at 500 is Ile. Note that I500L and I500V have a human-type metabolic pattern, suggesting that positional change or deletion of one methyl group can change the ratio between C-23 and C-24 oxidation pathways. The ratio between C-23 and C-24 oxidation pathways of I500T was estimated to be 0.16, which was much higher than that of wild type rat CYP24A1 (0.01) and significantly higher than T416M (0.08).

One of the most interesting findings in this study is the reaction specificity of the mutant I500F. In addition to 24*R*-hydroxylated (M5) and 23*S*-hydroxylated (M4) products, unknown product UK2 was observed as a major metabolite. Judging from its retention time in reversed-phase HPLC, UK2 is neither 26- nor 27-hydroxylated product. Two major metabolites of 1α,25(OH)$_2$D$_3$ by CYP3A4, which are considered to be 23*R*- and 24*S*-hydroxylated products, showed different retention times from UK2 (Xu *et al*., 2006). Based on these results, UK2 might have a hydroxyl group at a novel position such as C-22. Metabolic analysis and kinetic studies suggest that the substrate-binding pocket of I500F is quite different from those of both rat and human CYP24A1.

To our best knowledge, this is the first report showing the amino acid residues of CYP24A1 responsible for its reaction specificity. Naturally occurring one point mutation is adequate to change the ratio between C-23 and C-24 oxidation pathways. Such metabolites as 24*R*,25(OH)$_2$D$_3$ (Ornoy *et al*., 1978, Corvol *et al*., 1978, Henry and Norman, 1978) and 1α,25(OH)$_2$D$_3$-26,23-lactone (Shima *et al*., 1990) have been reported to be biologically active. Thus, the change of the ratio between C-23 and C-24 oxidation pathways appears to have biological significance.

Our findings indicate that the substitution of one nucleotide of rat CYP24A1 gene can produce human-type CYP24A1. Thus, it might be possible to generate a “humanized rat” on CYP24A1-dependent metabolism by homologous recombination. Humanized rats or mice would be useful to predict the metabolism of vitamin D analogs in humans.

Molecular Pharmacology Fast Forward. Published on April 14, 2006 as DOI: 10.1124/mol.106.023275
This article has not been copyedited and formatted. The final version may differ from this version.

References

Abe D, Sakaki T, Kusudo T, Kittaka A, Saito N, Suhara Y, Fujishima T, Takayama H, Hamamoto H, Kamakura, M., Ohta, M., and Inouye (2005) Metabolism of 2 alpha-propoxy-1 alpha,25-dihydroxyvitamin D_3 and 2 alpha-(3-hydroxypropoxy)-1 alpha,25-dihydroxyvitamin D_3 by human CYP27A1 and CYP24A1. *Drug Metab Dispos* **33**: 778-784

Akiyoshi-Shibata M, Sakaki T, Ohyama Y, Noshiro M, Okuda K, and Yabusaki Y (1994) Structure-function Relationships in the vitamin D endocrine system, *Eur J Biochem*.**224**: 335-343

Annalora A, Bobrovnikova-Marion E, Serda R, Lansing L, Chiu ML, Pastuszyn A, Iyer S, Marcus CB, Omdahl JL (2004) Rat cytochrome P450C24 (CYP24A1) and the role of F249 in substrate binding and catalytic activity. *Arch Biochem Biophys* **425**: 133-146.

Beckman MJ, Tadikonda P, Werner E, Prahl J, Yamada S, and DeLuca HF (1996) Human 25-hydroxyvitamin D_3-24-hydroxylase, a multicatalytic enzyme, *Biochemistry* **35**:8465-8472

Binderup L, Latini S, Binderup E, Bretting C, Calverley M, and Hansen K (1991) 20-epi-vitamin D_3 analogues: A novel class of potent regulators of cell growth and immune responses, *Biochem Pharmacol*.**42:** 1569-1575

Binderup L (1992) Immunological properties of vitamin D analogues and metabolites. Immunological properties of vitamin D analogues and metabolites, *Biochem. Pharmacol*. **43**: 1885-1892.

Boyle IT, Gray RW and DeLuca HF (1971) Regulation by calcium of in vivo synthesis of 1,25-dihydroxycholecalciferol and 21,25-dihydroxycholecalciferol. *Proc Natl Acad Sci. USA* **68**: 2131-2134.

Bouillon R, Okamura WH, and Norman AW (1995) Structure-function Relationships in the vitamin D endocrine system. *Endocr. Rev.* **16**: 200-257

Corvol, M. T., Dumontier, M. F., Garabedian, M., and Rappaport, R. (1978) Vitamin D and cartilage. II. Biological activity of 25-hydroxycholecaciferol and 24,25- and 1,25-dihydroxycholecaciferols cultured growth plate chondrocytes. *Endocrinology* **102**: 1269-1274

Dilorth, F.J., Williams, G..R., Kissmeyer, A.M., Nielsen, J.L., Binderup, E., Calverley, M.J., Makin, H.L., and Jones, G. (1997) The vitamin D analog KH1060, is rapidly degraded both in vivo and in vitro via several pathways: Principal metabolites generated retain significant biological activity. *Endocrinology* **138**: 5485-5496.

Gotoh O. (1992) Substrate recognition sites in cytochrome P450 family 2 (CYP2) proteins inferred from comparative analyses of amino acid and coding nucleotide sequences.

J Biol Chem **267**: 83-90.

Henry HL, and Norman AW (1978) Vitamin D: two dihydroxylated metabolites are required for normal chicken egg hatchability, *Science* **201**: 835-837

Hiwatashi A, Nishii Y, and Ichikawa,Y (1982) Purification of cytochrome P-450D 1α (25-hydroxyvitamin D_3-1α-hydroxylase) of bovine kidney mitochondria. *Biochem Biophys Res Commun*.**105**: 320-327

Holick MF, Schnoes HK, and DeLuca HF (1971) Identification of 1,25-dihydroxycholecalciferol, a form of vitamin D_3 metabolically active in the intestine. *Proc Natl Acad Sci USA* **68**: 803-804.

Kusudo T, Sakaki T, Abe D, Fujishima T, Kittaka A, Takayama H, Ohta M, and Inouye K (2003) Metabolism of 20-epimer of 1α,25-dihydroxyvitamin D_3 by CYP24, species-based difference between humans and rats. *Biochem Biophys Res Commun.***309**: 885-892

Kusudo T, Sakaki T, Abe D, Fujishima T, Kittaka A, Takayama H, Hatakeyama S, Ohta M, and Inouye K (2004) Metabolism of A-ring diastereomers of 1α,25- dihydroxyvitamin D_3 by CYP24A1. *Biochem Biophys Res Commun.* **321**: 774-782.

Kahraman M, Sinishtanj S., Dolan PM., Kebsler TW, Peleg S., Saha U., Chung SS., Bernstein G Korczak B., Posner GH. Potent, (2004) selective and low-calcemic inhibitors of CYP24 hydroxylase: 24-sulfoximine analogues of the hormone 1α,25-dihydroxyvitamin D(3). *J Med Chem.* **47**: 6854-6863.

Kondo S, Sakaki T, Ohkawa H, and Inouye K (1999) Electrostatic interaction between cytochrome P450 and NADPH-P450 reductase: comparison of mixed and fused systems consisting of rat cytochrome P450 1A1 and yeast NADPH-P450 reductase. *Biochem Biophys Res Commun.***257**: 273-278

Lawson DE, Fraser DR., Kodicek E, Morris HR, and Williams DH (1971) Identification of 1,25-dihydroxycholecalciferol, a new kidney hormone controlling calcium metabolism. *Nature* **230**: 228-230

Lowry OH, Rosebrough NJ, Farr AL, Randall RJ (1951) Protein measurement with the Folin phenol reagent. *J Biol Chem.***193**: 265-275

Nelson DR, Zeldin DC, Hoffman SM, Maltais LJ, Wain WH, Nebert DW (2004) Comparison of cytochrome P450 (CYP) genes from the mouse and human genomes, including nomenclature recommendations for genes, pseudogenes and alternative-splice variants. *Pharmacogenetics* **14**: 1-18

Norman, A.W., Myrtle J.F., Midgett, R.J., Nowicki, H.G. Williams, V. and Popjak G. (1971) 1,25-dihydroxycholecalciferol: identification of the proposed active form of vitamin D_3 in the intestine. *Science* **173**: 51-54.

Omdahl JL, Bobrovnikova EV, Annalora A, Chen P, Serda R, (2003) Expression,

structure-function, and molecular modeling of vitamin D P450s. *J Cell Biochem* **88**: 356-362

Omura T, and Sato R (1964) The carbon monoxide-binding pigment of liver microsomes. *J Biol Chem* **239**: 2379-2385

Ornoy A, Goodwin D, Noff D, and Edelstein S (1978) 24, 25-dihydroxyvitamin D is a metabolite of vitamin D essential for bone formation, *Nature* **276**: 517-519

Portale AA, and Miller WL (2000) Human 25-hydroxyvitamin D-1α-hydroxylase: cloning, mutations, and gene expression. *Pediatr Naphrol* **14**: 620-625.

Rowland P, Blaney FE, Smyth MG, Jones JJ, Leydon VR, Oxbrow AK, Lewis CJ, Tennant MG, Modi S, Eggleston DS, Chenery RJ, and Bridges AM (2006) Crystal Structure of Human Cytochrome P450 2D6, *J Biol Chem*. 281, 7614-7622

Sakaki T, Sawada N, Nonaka Y, Ohyama Y,and Inouye K (1999) Metabolic studies using recombinant Escherichia coli cells producing rat mitochondrial CYP24, *Eur J Biochem* **262**: 43-48

Sakaki T, Sawada N, Komai K, Shiozawa S, Yamada S, Yamamoto K, Ohyama Y, and Inouye K (2000) Dual metabolic pathway of 25-hydroxyvitamin D_3 catalyzed by human CYP24. *Eur J Biochem* **267**: 6158-6165.

Sakaki T, Sawada N, Abe D, Komai K, Shiozawa S, Nonaka Y, Nakagawa K, Okano T, Ohta M, Inouye K (2003) 26,26,26,27,27,27-F_6-1α, 25-dihydroxyvitamin D_3 by CYP24: species-based difference between humans and rats, *Biochem Pharmacol* **65**: 1957-1965

Sawada N, Kusudo T, Sakaki T, Hatakeyama S, Hanada M, Abe D, Kamao M, Okano T, Ohta M, Inouye K. (2004) Novel metabolism of 1 α,25-dihydroxyvitamin D_3 with C24-C25 bond cleavage catalyzed by human CYP24A1, *Biochemistry* 43, 4530-4537

Scott EE, He YA, Wester MR, White MA, Chin CC, Halpert JR., Johnson EF, Stout CD (2003) An open conformation of mammalian cytochrome P450 2B4 at 1.6-A resolution. *Proc Natl Acad Sci. U S A* **100**: 13196-13201

Schoch GA, Yano JK, Wester MR, Griffin KJ, Stout CD, and Johnson EF. (2004) Structure of human microsomal cytochrome P450 2C8: Evidence for a peripheral fatty acid binding site. *J. Biol. Chem*. 279, 9497-9503

Schuster I, Egger H, Nussbaumer P, Kroemer RT (2003) Inhibitors of vitamin D hydroxylases: structure-activity relationships. *J Cell Biochem*. **88**: 372-380.

Shima M, Tanaka H, Norman AW, Yamaoka K, Yoshikawa H, Takaoka K, Ishizuka S, and Seino Y (1990) 23(S),25(R)-1,25-dihydroxyvitamin D_3-26,23-lactone stimulates murine bone formation in vivo. *Endocrinology* **126**: 832-836

Uchida E, Kagawa N, Sakaki T, Urushino N, Sawada N, Kamakura M, Ohta M, Kato S, Inouye K. (2004) Purification and characterization of mouse CYP27B1 overproduced by an

Escherichia coli system coexpressing molecular chaperonins GroEL/ES. *Biochem Biophys Res Commun.* **323**: 505-511.

Wester MR., Johnson EF, Marques-Soares C, Dansette PM, Mansuy D, Stout C (2003) Structure of a substrate complex of mammalian cytochrome P450 2C5 at 2.3 A resolution: evidence for multiple substrate binding modes, *Biochemistry* **42**: 6370-6379

Williams PA, Cosme J, Sridhar V, Johnson EF, and McRee DE (2000) Mammalian microsomal cytochrome P450 monooxygenase: structural adaptations for membrane binding and functional diversity. *Mol Cell.* **5**: 121-131

Williams PA, Cosme J, Ward A, Angove H, Matak C, Vinkovic D, Jhoti H (2003) Crystal structure of human cytochrome P450 2C9 with bound warfarin. *Nature* **424**: 464-468

Williams PA, Cosme J, Vinkovic DM, Ward A, Angove HC, Day PJ, Vonrhein C, Tickle IJ, Jhoti H (2004) Crystal structures of human cytochrome P450 3A4 bound to metyrapone and progesterone. *Science* **305**: 683-686.

Xu Y, Hashizume T, Shuhart MC, Davis CL, Nelson WL, Sakaki T, Kalhorn TF, Watkins PB, Schuetz EG, and Thummel KE (2006) Intestinal and hepatic CYP3A4 catalyze hydroxylation of 1α,25-dihydroxyvitamin D_3: implications for drug-induced osteomalacia, *Mol Pharmacol*. 69, 56-65

Yamamoto K, Masuno H, Sawada N, Sakaki T, Inouye K, Ishiguro M, and Yamada S (2004) Homology modeling of human 25-hydroxyvitamin D_3 1α-hydroxylase (CYP27B1) based on the crystal structure of rabbit CYP2C5, *J Steroid Biochem Mol Biol* **89-90**: 167-171

Yamamoto K, Uchida E, Urushino N, Sakaki T, Kagawa N, Sawada N, Kamakura M, Kato S, Inouye K, and Yamada S (2005) Identification of the amino acid residue of CYP27B1 responsible for binding of 25-hydroxyvitamin D_3 whose mutation causes vitamin D-dependent rickets type 1. *J Biol Chem* **280**: 30511-30516

Yano JK, Hsu M, Griffin KJ, Stout CD, and Jhonson EF (2005) Structure of human microsomal cytochrome P450 2A6 complexed with coumarin and methoxsalen. *Nat Struct Mol Biol*. 12, 822-823.

Molecular Pharmacology Fast Forward. Published on April 14, 2006 as DOI: 10.1124/mol.106.023275
This article has not been copyedited and formatted. The final version may differ from this version.

Footnotes

*This work was supported in part by a Grant-in-Aid for Scientific Research from the Ministry of Education, Science and Culture of Japan, and Sankyo Foundation of Life Sciences.

Toshiyuki Sakaki
Biotechnology Research Center,
Faculty of Engineering, Toyama Prefectural University,
5180 Kurokawa, Imizu, Toyama 939-0398, Japan

Molecular Pharmacology Fast Forward. Published on April 14, 2006 as DOI: 10.1124/mol.106.023275
This article has not been copyedited and formatted. The final version may differ from this version.

FIGURE LEGENDS

Fig. 1. Alignment of the sequences of human CYP24A1 (hCYP24A1) and rat CYP24A1 (rCYP24A1).

The locations and names of the helices (designated with bars) and β sheets (designated with broken bars) are shown based on the three-dimensional model. Substrate recognition sites proposed by Gotoh (1992) are in light shading, and the locations of the mutated amino-acid residues are in dark shading.

Fig. 2. Metabolic pathways of 1α,25$(OH)_2D_3$ catalyzed by CYP24A1.

Numbers indicate the metabolites shown in Figs. 3 and 4.

Fig. 3. HPLC profiles of 1α,25$(OH)_2D_3$ and its metabolites by rat CYP24A1 (A), human CYP24A1 (B), and Thr416 mutants of rat CYP24A1 (C-H).

After incubation with 2.0 μM of 1α,25$(OH)_2D_3$ in the presence of 2.0 μM ADERENODOXIN and 0.2 μM ADR for 30 min, the reaction mixture was extracted and analyzed by the reverse phase HPLC as described in Material and Methods. Numbers indicate the metabolites in C-23 (red) and C-24 (blue) oxidation pathways, as shown in Fig.2.

Fig. 4. HPLC profiles of 1α,25$(OH)_2D_3$ and its metabolites by rat CYP24A1 and Ile500 mutants.

After incubation with 2.0 μM of 1α,25$(OH)_2D_3$ in the presence of 2.0 μM ADERENODOXIN and 0.2 μM ADR for 30 min, the reaction mixture was extracted and analyzed by the reverse phase HPLC as described in Material and methods. Numbers indicate the metabolites in C-23 (red) and C-24 (blue) oxidation pathways, as shown in Fig.2.

Fig. 5. Complex model of rat CYP24A1 and 1α,25$(OH)_2D_3$ represented by ribbon-loop drawing (A), and putative location of 1α,25$(OH)_2D_3$ and the amino acid residues, Thr416 and Ile500, in the substrate-binding pocket based on three-dimensional model of rat CYP24A1(B). Thr416 and Ile500 were located near the A-ring and triene part, respectively.

The distances between the amino acid residues and the substrate 1α,25$(OH)_2D_3$ are indicated.

Fig. 6. Normal phase HPLC profiles of the metabolites of 1α,25$(OH)_2D_3$ by human CYP24A1 (A) and rat CYP24A1 mutant, I500F (B).

The metabolites eluted at about 18 minutes with reverse phase HPLC (Fig. 3-F) were collected, and analyzed using normal-phase HPLC as described in Material and methods.

Molecular Pharmacology Fast Forward. Published on April 14, 2006 as DOI: 10.1124/mol.106.023275
This article has not been copyedited and formatted. The final version may differ from this version.

23*S*(OH), 24*R*(OH), UK1, and UK2 indicate 1α,23*S* ,25$(OH)_3D_3$, 1α,24*R* ,25$(OH)_3D_3$, unknown metabolites 1 and 2, respectively.

Molecular Pharmacology Fast Forward. Published on April 14, 2006 as DOI: 10.1124/mol.106.023275
This article has not been copyedited and formatted. The final version may differ from this version.

Table1 Oligonucleotides used to generate CYP24A1 mutants

Mutation	Oligonucleotides
H125Y	5'-ACAGAGAGCGCGTATCCCCAGCGACTG-3'
	5'-CAGTCGCTGGGGATACGCGCTCTCTGT-3'
H140Y	5'-GGAAAGCCTATCGCGACTACAGGAACGAAG-3'
	5'-CTTCGTTCCTGTAGTCGCGATAGGCTTTCC-3'
N142K	5'-CTATCGCGACCACAGGAAAGAAGCCTACG-3'
	5'-CGTAGGCTTCTTTCCTGTGGTCGCGATAG-3'
R262S	5'-GTTGCACAAGAGCCTCAACACCAAAG-3'
	5'-CTTTGGTGTTGAGGCTCTTGTGCAAC-3'
A270D	5'-CAAAGTGTGGCAGGACCATACGCTG-3'
	5'-CAGGCGTATGGTCCTGCCACACTTTG-3'
T416M	5'-GGAACAGTGTTAATGCTCAATACCCA-3'
	5'-TGGGTATTGAGCATTAACACTGTTCC-3'
T416A	5'-GGAACAGTGTTAGCCCTCAATACCCA-3'
	5'-TGGGTATTGAGGGCTAACACTGTTCC-3'
T416S	5'-GGAACAGTGTTAAGCCTCAATACCCA-3'
	5'-TGGGTATTGAGGCTTAACACTGTTCC-3'
T416V	5'-GGAACAGTGTTAGTCCTCAATACCCA-3'
	5'-TGGGTATTGAGGACTAACACTGTTCC-3'
T416I	5'-GGAACAGTGTTAATCCTCAATACCCA-3'
	5'-TGGGTATTGAGGATTAACACTGTTCC-3'
T416F	5'-GGAACAGTGTTATTCCTCAATACCCA-3'
	5'-TGGGTATTGAGGAATAACACTGTTCC-3'
L498S	5'-GATGCTGCACTCTGGCATCCTG-3'
	5'-CAGGATGCCAGAGTGCAGCATC-3'
I500T	5'-CTTGGCACCCTGGTACCC-3'
	5'-TACCAGGGTGCCAAGGTG-3'
I500A	5'-CTTGGCGCCCTGGTACCC-3'
	5'-TACCAGGGCGCCAAGGTG-3'
I500V	5'-CTTGGCGTCCTGGTACCC-3'
	5'-TACCAGGACGCCAAGGTG-3'
I500L	5'-CTTGGCCTCCTGGTACCC-3'
	5'-TACCAGGAGGCCAAGGTG-3'
I500F	5'-CTTGGCTTCCTGGTACCC-3'
	5'-TACCAGGAAGCCAAGGTG-3'

Molecular Pharmacology Fast Forward. Published on April 14, 2006 as DOI: 10.1124/mol.106.023275
This article has not been copyedited and formatted. The final version may differ from this version.

Table 2. The ratio of C-23 to C-24 oxidation pathways

CYP24A1	C-23/C-24
rat	0.01
T416A	0.01
T416S	0.01
T416M	0.08
T416V	0.16
T416 I	0.19
T416F	0.12
I 500A	0.15
I 500V	0.13
I 500T	0.16
I 500L	0.16
Human	0.27

The ratio between the summed products of C-23 pathway (M1, M4, M7) and those of C-24 pathway (M2, M3, M5, M6) is indicated.

Molecular Pharmacology Fast Forward. Published on April 14, 2006 as DOI: 10.1124/mol.106.023275
This article has not been copyedited and formatted. The final version may differ from this version.

Table 3. Kinetic parameters of wild type and mutants CYP24A1 for 1α,25(OH)$_2$D$_3$

CYP24A1	Type	K_m (μM)	k_{cat} (min^{-1})	k_{cat} /K_m
rat WT	R	0.19±0.08	0.26±0.10	1.4±0.1
human WT	H	0.35±0.02	0.43±0.04	1.2±0.1
T416A	R	0.24±0.10	0.25±0.07	1.2±0.3
T416S	R	0.22±0.01	0.30±0.02	1.4±0.1
T416V	H	1.04±0.32	0.72±0.31	0.71±0.31
T416M	H	0.66±0.06	0.21±0.09	0.32±0.15
I 500T	H	0.14±0.04	0.12±0.03	0.92±0.07
I 500L	H	0.30±0.12	0.05±0.01	0.17±0.03
I 500F	N	1.14±0.40	0.11±0.04	0.10±0.04

R, H, and N indicate rat-, human-, and novel-type metabolism, respectively.

The reaction was performed in the presence of 0.1 μM of adrenodoxin, 0.01 μM of ADR as described in Materials and methods. Under these conditions, the sum of 23*S*-hydroxylated (M4) and 24*R*-hydroxylated (M5) products is more than 90 % of total metabolites.

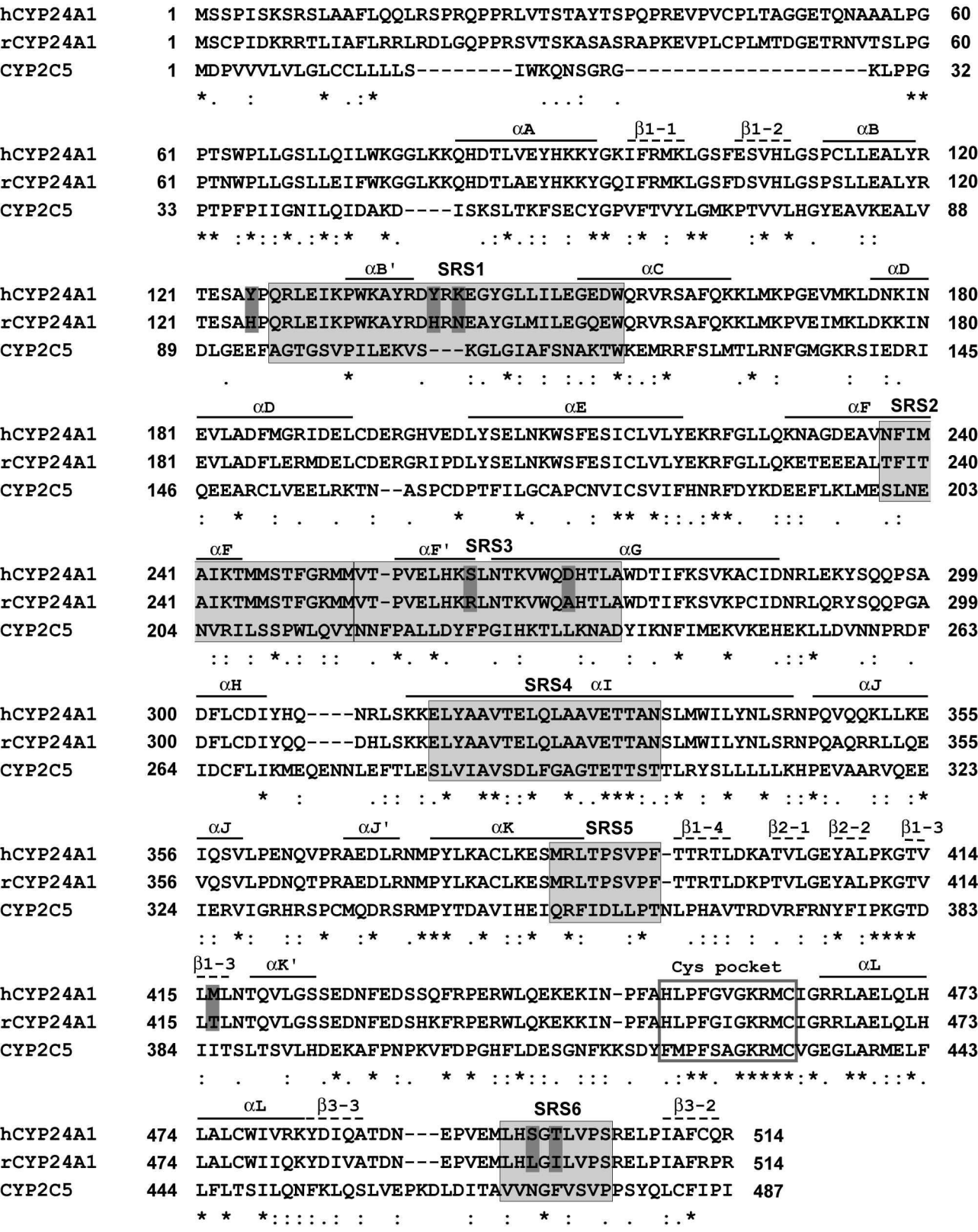
hCYP24A1 1 MSSPISKSRSLAAFLQQLRSPRQPPRLVTSTAYTSPQPREVPVCPLTAGGETQNAAALPG 60
rCYP24A1 1 MSCPIDKRRTLIAFLRRLRDLGQPPRSVTSKASASRAPKEVPLCPLMTDGETRNVTSLPG 60
CYP2C5 1 MDPVVVLVLGLCCLLLLS--------IWKQNSGRG--------------------KLPPG 32
αA β1-1 β1-2 αB
hCYP24A1 61 PTSWPLLGSLLQILWKGGLKKQHDTLVEYHKKYGKIFRMKLGSFESVHLGSPCLLEALYR 120
rCYP24A1 61 PTNWPLLGSLLEIFWKGGLKKQHDTLAEYHKKYGQIFRMKLGSFDSVHLGSPSLLEALYR 120
CYP2C5 33 PTPFPIIGNILQIDAKD----ISKSLTKFSECYGPVFTVYLGMKPTVVLHGYEAVKEALV 88
αB' SRS1 αC αD
hCYP24A1 121 TESAYPQRLEIKPWKAYRDYRKEGYGLLILEGEDWQRVRSAFQKKLMKPGEVMKLDNKIN 180
rCYP24A1 121 TESAHPQRLEIKPWKAYRDHRNEAYGLMILEGQEWQRVRSAFQKKLMKPVEIMKLDKKIN 180
CYP2C5 89 DLGEEFAGTGSVPILEKVS---KGLGIAFSNAKTWKEMRRFSLMTLRNFGMGKRSIEDRI 145
αD αE αF SRS2
hCYP24A1 181 EVLADFMGRIDELCDERGHVEDLYSELNKWSFESICLVLYEKRFGLLQKNAGDEAVNFIM 240
rCYP24A1 181 EVLADFLERMDELCDERGRIPDLYSELNKWSFESICLVLYEKRFGLLQKETEEEALTFIT 240
CYP2C5 146 QEEARCLVEELRKTN--ASPCDPTFILGCAPCNVICSVIFHNRFDYKDEEFLKLMESLNE 203
αF αF' SRS3 αG
hCYP24A1 241 AIKTMMSTFGRMMVT-PVELHKSLNTKVWQDHTLAWDTIFKSVKACIDNRLEKYSQQPSA 299
rCYP24A1 241 AIKTMMSTFGKMMVT-PVELHKRLNTKVWQAHTLAWDTIFKSVKPCIDNRLQRYSQQPGA 299
CYP2C5 204 NVRILSSPWLQVYNNFPALLDYFPGIHKTLLKNADYIKNFIMEKVKEHEKLLDVNNPRDF 263
αH SRS4 αI αJ
hCYP24A1 300 DFLCDIYHQ----NRLSKKELYAAVTELQLAAVETTANSLMWILYNLSRNPQVQQKLLKE 355
rCYP24A1 300 DFLCDIYQQ----DHLSKKELYAAVTELQLAAVETTANSLMWILYNLSRNPQAQRRLLQE 355
CYP2C5 264 IDCFLIKMEQENNLEFTLESLVIAVSDLFGAGTETTSTTLRYSLLLLLKHPEVAARVQEE 323
αJ αJ' αK SRS5 β1-4 β2-1 β2-2 β1-3
hCYP24A1 356 IQSVLPENQVPRAEDLRNMPYLKACLKESMRLTPSVPF-TTRTLDKATVLGEYALPKGTV 414
rCYP24A1 356 VQSVLPDNQTPRAEDLRNMPYLKACLKESMRLTPSVPF-TTRTLDKPTVLGEYALPKGTV 414
CYP2C5 324 IERVIGRHRSPCMQDRSRMPYTDAVIHEIQRFIDLLPTNLPHAVTRDVRFRNYFIPKGTD 383
β1-3 αK' Cys pocket αL
hCYP24A1 415 LMLNTQVLGSSEDNFEDSSQFRPERWLQEKEKIN-PFAHLPFGVGKRMCIGRRLAELQLH 473
rCYP24A1 415 LTLNTQVLGSSEDNFEDSHKFRPERWLQKEKKIN-PFAHLPFGIGKRMCIGRRLAELQLH 473
CYP2C5 384 IITSLTSVLHDEKAFPNPKVFDPGHFLDESGNFKKSDYFMPFSAGKRMCVGEGLARMELF 443
αL β3-3 SRS6 β3-2
hCYP24A1 474 LALCWIVRKYDIQATDN---EPVEMLHSGTLVPSRELPIAFCQR 514
rCYP24A1 474 LALCWIIQKYDIVATDN---EPVEMLHLGILVPSRELPIAFRPR 514
CYP2C5 444 LFLTSILQNFKLQSLVEPKDLDITAVVNGFVSVPPSYQLCFIPI 487

Fig. 1

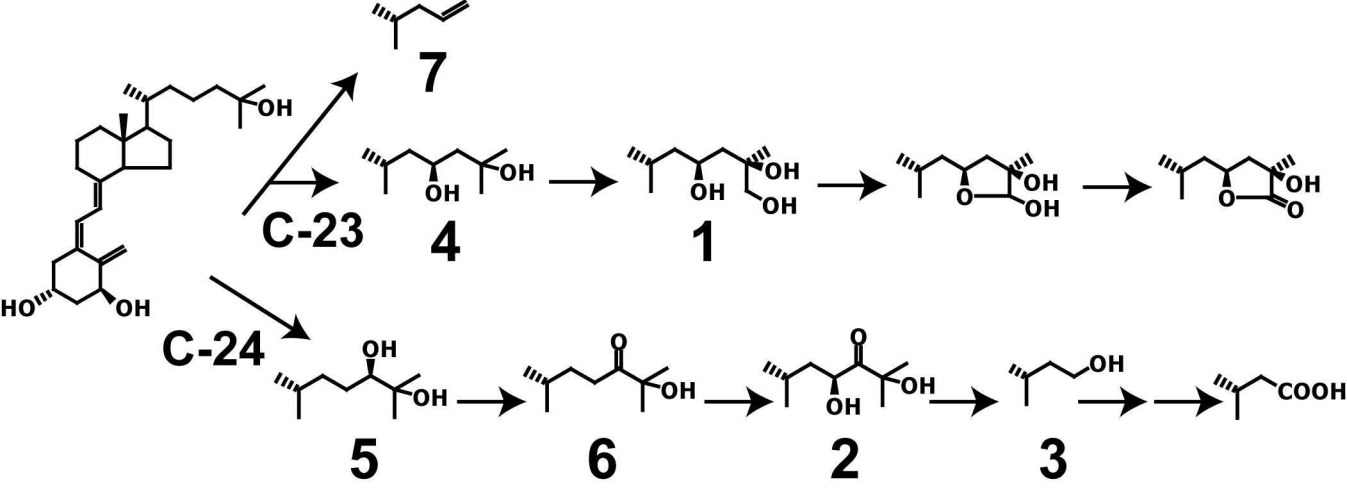

Fig. 2

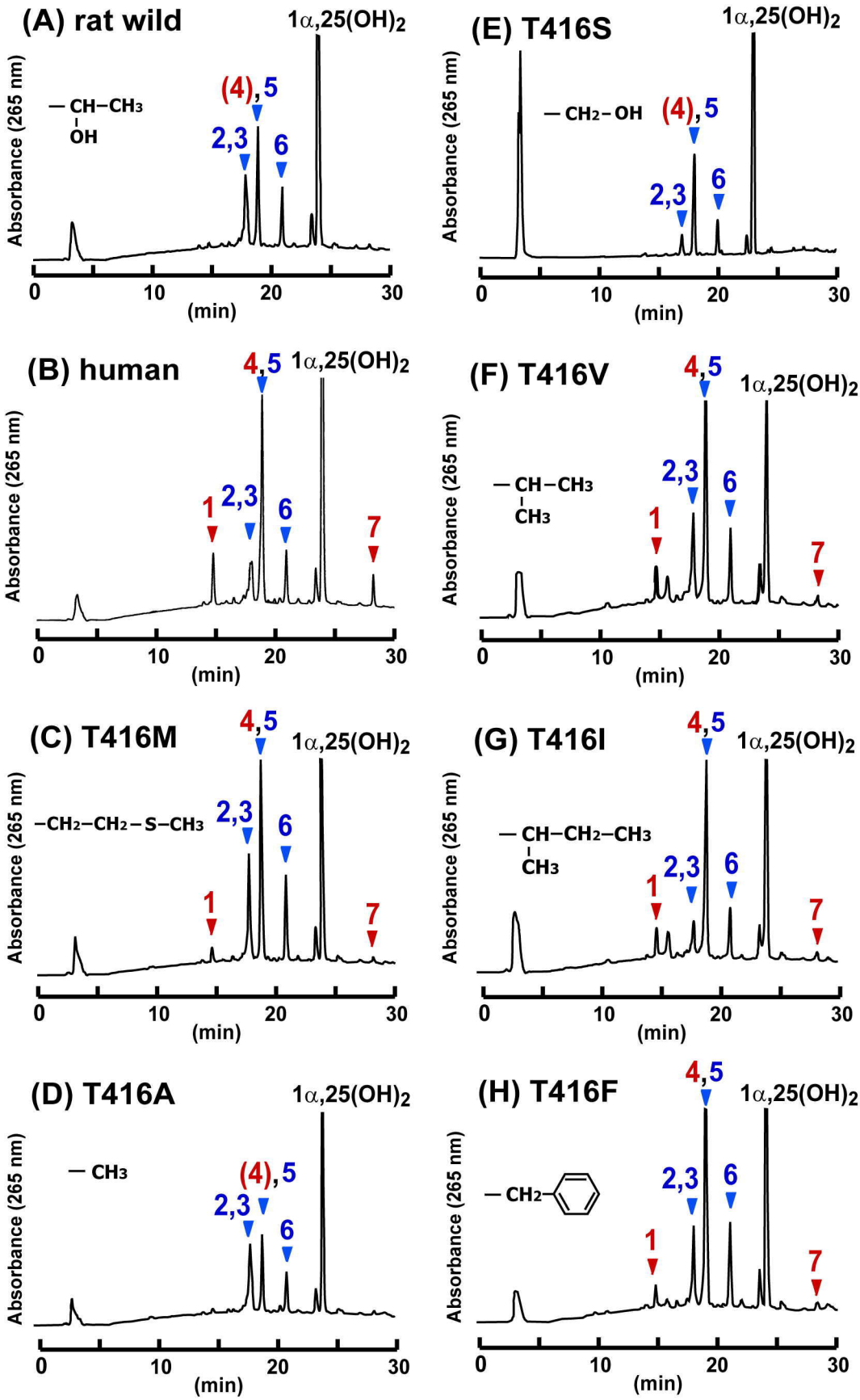
(A) rat wild
1α,25(OH)2
— CH–CH3
OH
(4),5
2,3
6
Absorbance (265 nm)
0
10
20
30
(min)
(E) T416S
1α,25(OH)2
— CH2–OH
(4),5
2,3
6
Absorbance (265 nm)
0
10
20
30
(min)
(B) human
4,5
1α,25(OH)2
1
2,3
6
7
Absorbance (265 nm)
0
10
20
30
(min)
(F) T416V
4,5
1α,25(OH)2
— CH–CH3
CH3
2,3
6
1
7
Absorbance (265 nm)
0
10
20
30
(min)
(C) T416M
4,5
1α,25(OH)2
–CH2–CH2–S–CH3
2,3
6
1
7
Absorbance (265 nm)
0
10
20
30
(min)
(G) T416I
4,5
1α,25(OH)2
— CH–CH2–CH3
CH3
2,3
6
1
7
Absorbance (265 nm)
0
10
20
30
(min)
(D) T416A
1α,25(OH)2
— CH3
(4),5
2,3
6
Absorbance (265 nm)
0
10
20
30
(min)
(H) T416F
4,5
1α,25(OH)2
— CH2–
2,3
6
1
7
Absorbance (265 nm)
0
10
20
30
(min)

Fig. 3

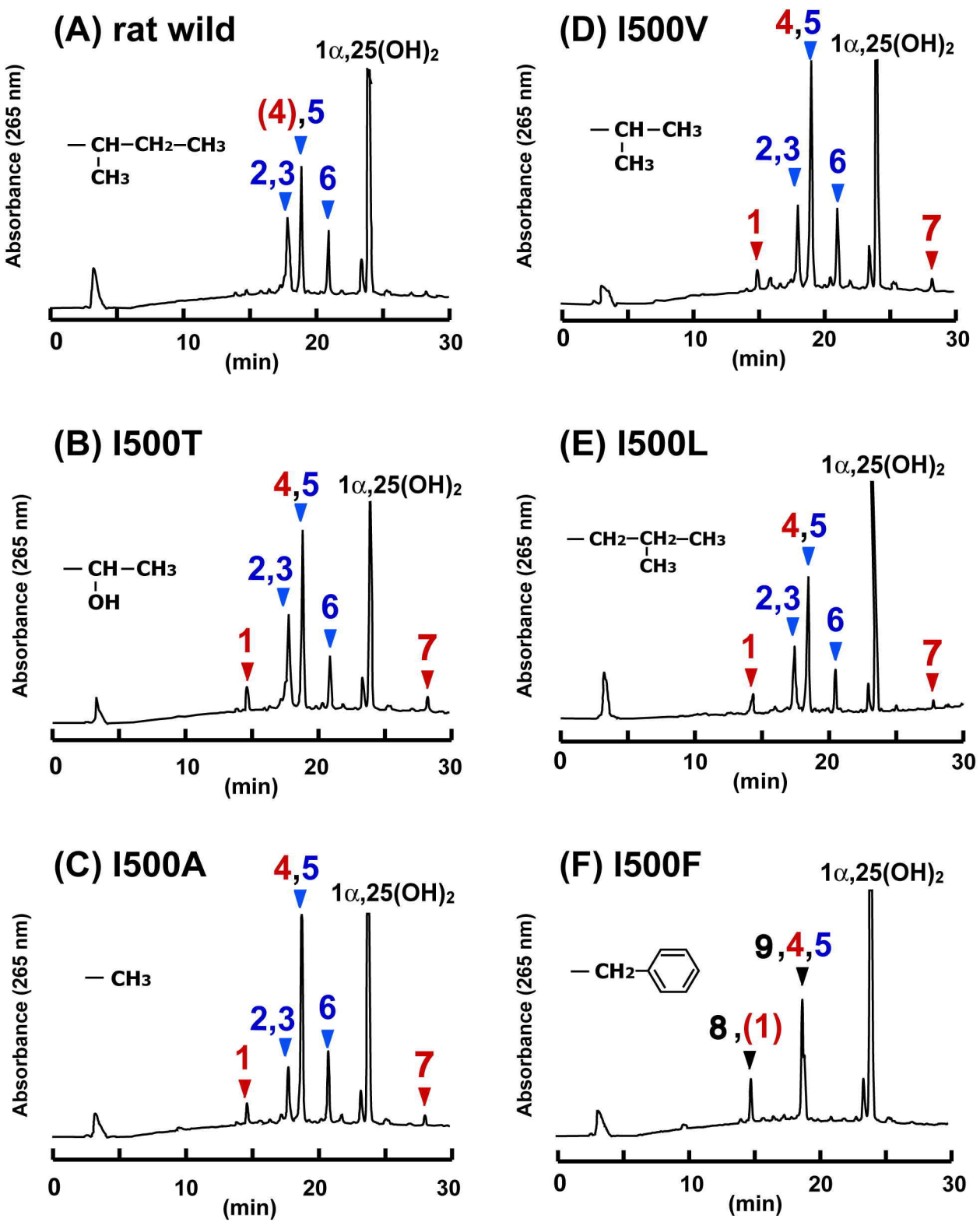
(A) rat wild
1α,25(OH)2
(4),5
2,3
6
— CH–CH2–CH3
CH3
Absorbance (265 nm)
0
10
20
30
(min)
(D) I500V
4,5
1α,25(OH)2
2,3
6
1
7
— CH–CH3
CH3
(B) I500T
4,5
1α,25(OH)2
2,3
6
1
7
— CH–CH3
OH
(E) I500L
1α,25(OH)2
4,5
2,3
6
1
7
— CH2–CH2–CH3
CH3
(C) I500A
4,5
1α,25(OH)2
2,3
6
1
7
— CH3
(F) I500F
1α,25(OH)2
9,4,5
8,(1)
— CH2

Fig. 4

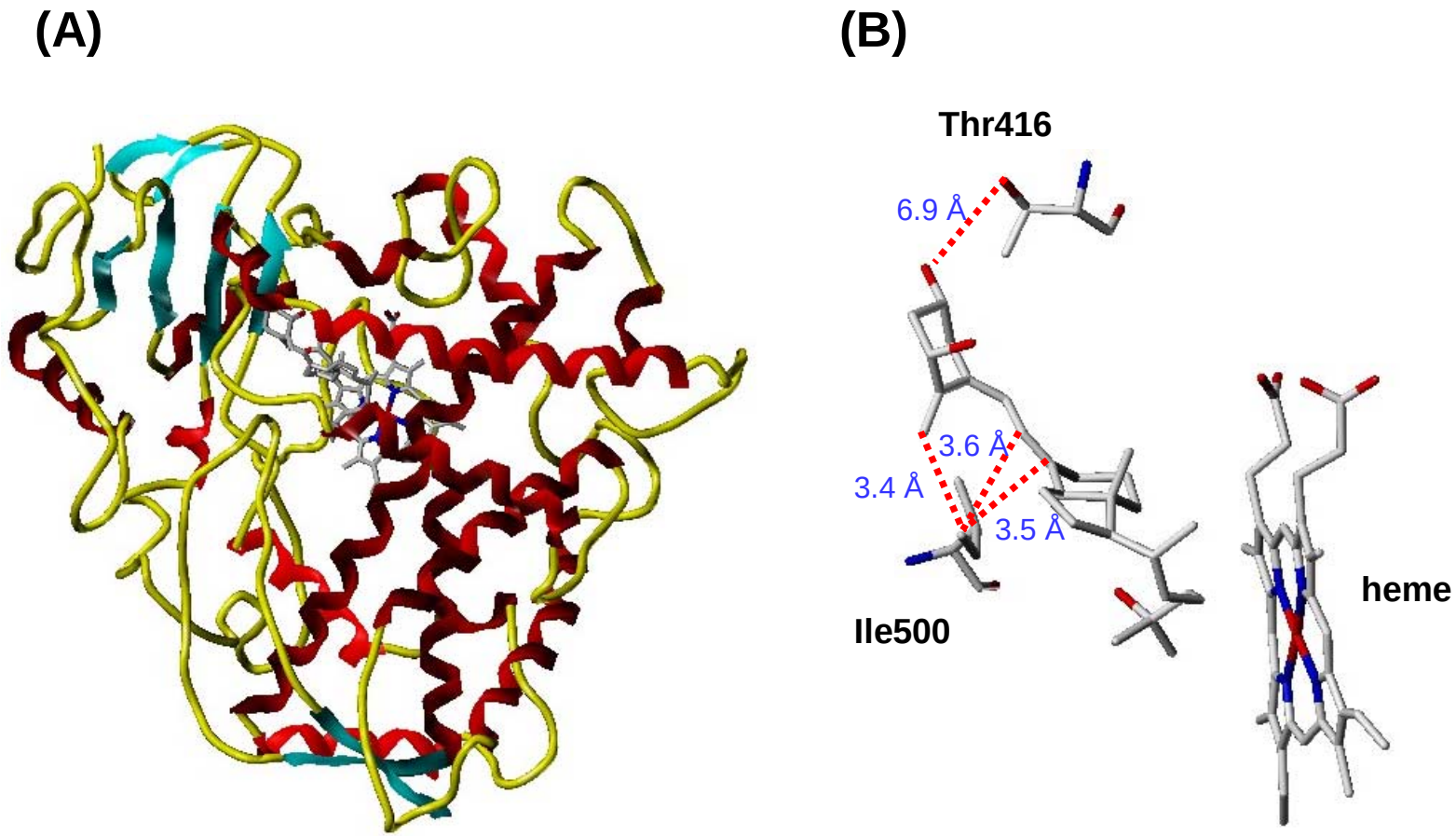

Fig. 5

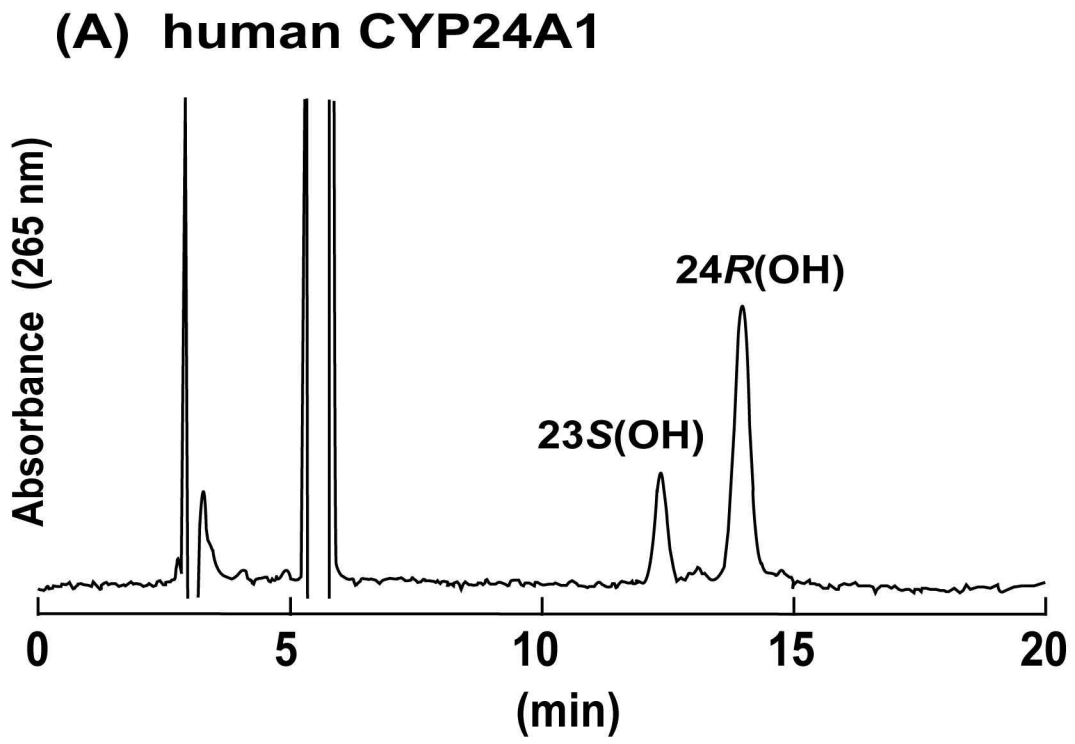
(A) human CYP24A1
Absorbance (265 nm)
24R(OH)
23S(OH)
0
5
10
15
20
(min)

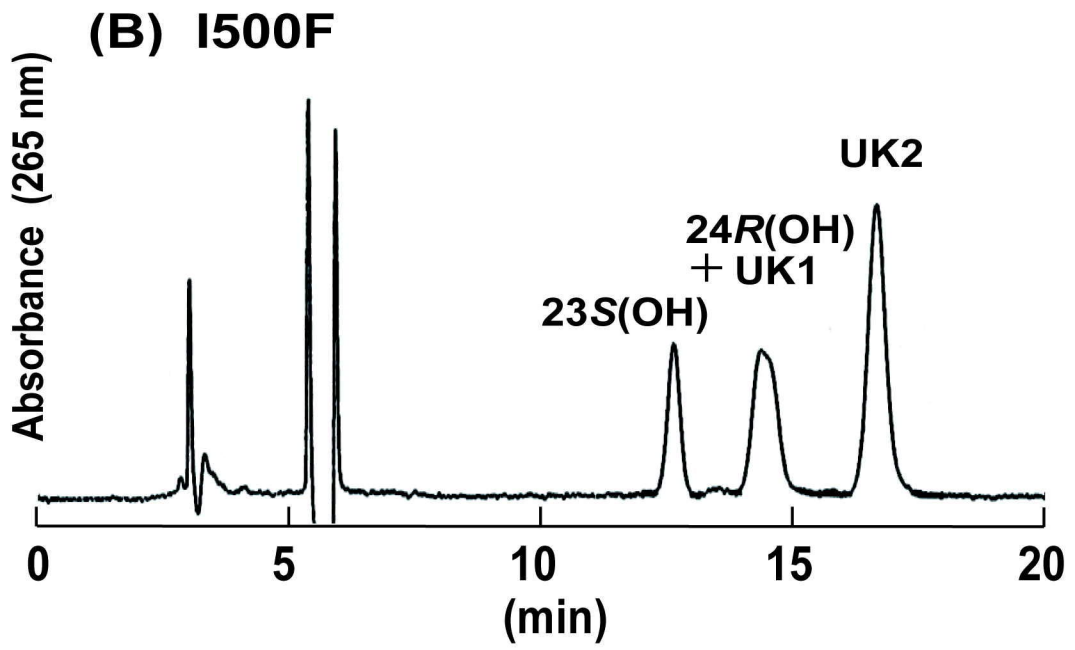
(B) I500F
Absorbance (265 nm)
UK2
24R(OH)
+ UK1
23S(OH)
0
5
10
15
20
(min)

Fig. 6